Automated Assessment of Ghost Artifacts in MRI

S. A. Tsaftaris[1,2], X. Zhou[2], and R. Dharmakumar[2]

[1]Electrical Engineering and Computer Science, Northwestern University, Evanston, IL, United States, [2]Radiology, Northwestern University, Chicago, IL, United States

Introduction: Flow artifacts in MR images can appear as image ghosts within and outside the body cavity. Technical improvements aimed at suppressing these image ghosts often rely on expert scoring (1,2) or on semi-automated methods demanding tissue segmentation and estimation of statistical properties of intensity distribution (3) to evaluate the efficacy of the methods. These approaches can be labor intensive, introduce observer bias, computationally demanding, and error-prone if tissue segmentation is used. Herein we propose two fully automated image-processing methods that rely on the statistical properties of background (noise) pixels to assess the presence of flow artifacts (appearing as image ghosts) without requiring tissue segmentation. The first method rapidly evaluates the presence of flow artifacts in a global fashion, while the second one provides a more detailed characterization of the artifacts. We evaluate the proposed methods in the setting of cardiac phase-resolved myocardial blood-oxygen-level-dependent (BOLD) MRI where different cine SSFP imaging strategies are proposed for overcoming flow artifacts. Finally we assess the utility of our automated approaches against expert scoring results.

Methods: <u>Imaging Studies</u>: Six healthy dogs were studied in a Siemens 1.5T scanner using three different breath-held 2D SSFP cine sequences with known flow artifact properties. Imaging was prescribed in the basal position along the short axis, where flow artifacts are most pronounced: (A) Conventional 2D cine SSFP (Repetition Time (TR, ms) / Bandwidth (BW, Hz/pixel) = 3.5/930, conventional cine SSFP with negligible myocardial BOLD sensitivity); (B) Standard long TR cine SSFP used for myocardial BOLD MRI (TR/BW = 6.2/239, optimal BOLD sensitivity with significant flow artifacts); and (C) Long TR cine SSFP with flow compensation for myocardial BOLD (TR/BW = 6.2/930, optimal BOLD sensitivity with expected reduction in flow artifacts). Scan parameters were: spatial resolution = $1.2 \times 1.2 \times 5$ mm^3, flip angle=70°, temporal resolution = 10-12ms, and no image acceleration (parallel imaging). <u>Image Processing</u>: Each cine study/stack $I(x,y,t)$ (t denotes cardiac phase) was loaded in Matlab and the per-pixel mean (I_A) and variance (I_V) were found across t. A level-set method (4) was used to segment the body from the surrounding background in I_A, initialized with a rectangle the size of I_A. A contour is evolved until it converged to the body-air interface, providing a binary mask M (M=1 for air outside the body, 0 otherwise). *Kurtosis-based Method*: The image $I_R=I_V/(I_A)^2$ (pixel-wise division) is found and all values in I_R in air (M=1) were collected to estimate the excess kurtosis (γ) of their distribution. We define $Q_K=\gamma$ to quantify the presence of flow artifacts. *Segmentation-based Method*: The pixel values of the image $I(x,y,t)/I_A$ (image is divided by I_A) in air (M=1) were collected and Rician and non-central Student's t models were fitted on their distribution (the Akaike Information Criterion (AIC) is used as goodness-of-fit.) The threshold $T=\mu+\sigma$ was defined, where μ, σ, are the mean and standard deviation (std) parameters of the best model. Artifact pixels in each image were identified as those with intensity > T. Following a 2x2 morphological dilation, the estimated total artifactual area (number of pixels) was recorded as n_f. To estimate noise parameters, artifact regions were excluded from the image and the same models were refitted. The metric $Q_S(t)$ was defined as $Q_S(t)=(\mu_f-\mu_b)/\sigma_b \cdot (n_f/n_M)$, where μ_f and n_f are the mean intensity and total area of the artifacts, respectively; μ_b and σ_b, are the mean and std respectively of the best model (based on AIC); and n_M is the number of pixels in air. For each stack, the mean (Q_{S1}), std (Q_{S2}), and maximum (Q_{S3}) of $Q_S(t)$ over all t were recorded. <u>Data Analysis:</u> Three expert reviewers, blinded to the sequence used, scored 16 studies for the presence of ghost artifacts between 1 (least) to 5 (most). Kruskal-Wallis ANOVA with Tukey-Post Hoc analysis was used to test for the presence of statistical difference in scores/metrics among the sequences. The metrics were correlated with Q_H (median choice of reviewers) to assess accuracy. Statistical significance was set at P<0.05.

Results: Fig. 1 shows results from a study with long TR (sequence B), where the artifacts were expected to be greater compared to those from images acquired with sequences A or C. The arrows in Fig. 1 demonstrate that I_R retains artifact information and that the segmentation method (Fig. 1d) accurately identifies the artifacts of Fig. 1a. Fig. 2 shows a composite of bar plots (mean ± standard error) for each imaging sequence and scoring method. Statistical comparisons of scores from most of the automated methods identified a difference in the presence of ghost artifacts in images acquired with sequences A and B or B and C, and were in full agreement with the expert findings. Only Q_{S1} failed to distinguish a quality difference among A and B, against expert findings. Regression analysis showed that Q_K had a strong correlation with Q_{S2} (0.83, P<0.01) and Q_{S3} (0.76, P<0.01) but not with Q_{S1} (0.5, P>0.1). The correlation of Q_H with Q_K, Q_{S1}, Q_{S2}, and Q_{S3}, was 0.7, 0.8, 0.92, and 0.93, respectively (all P<0.01).

Discussion & Conclusions: Two automated approaches for estimating ghost artifacts in cardiac cine images were presented. Results showed a strong agreement with expert findings. Regressions showed that the kurtosis-based method (Q_K) can assess the variability of artifact presence in a stack without processing each image separately as needed for Q_{S2}. It also showed that human observers are more likely to score for spurious and/or large artifact presence (strong correlation of Q_H with Q_{S2} and Q_{S3}.) We anticipate that such automated methods could replace the time consuming and possibly biased step of expert evaluation. In contrast to other methods (3), the proposed approaches (i) combine high order statistics (kurtosis) and model fitting to estimate the parameters; (ii) utilize the Student t model's robustness to outliers (artifacts) and ability to approximate other distributions as an alternative to the Rician distribution; and (iii) offer increased robustness against bias by dividing with the mean image (I_A). Although further studies are needed, multiple applications of these methods may be possible. First, the kurtosis approach may be useful to readily assess image quality in a clinical/research setting. Next, in a technical development setting, given the shear volume of images, it becomes unreasonable to expect experts to score the image stacks whenever new pulse sequences are tested. Thus, given the accuracy of the segmentation method (combining artifact-contrast-to-noise and area measurements) reproducible and unbiased estimates of ghost artifacts may be ascertained. Although the current study only tested the cine SSFP approaches, it is anticipated that the proposed methods could be tested whenever an unbiased and automated assessment of ghost artifacts is sought.
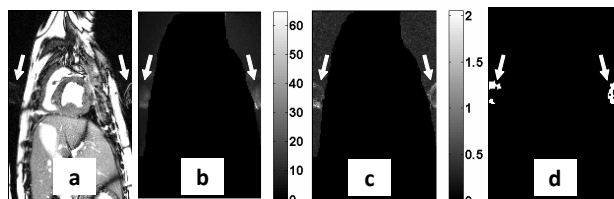
Fig. 1 a: An image acquired with sequence B; **b:** I_A (mean of 55 images) used by both methods; **c:** I_R image (Q_K=21); and **d:** artifacts of **a**, as detected with the segmentation method (Q_S(22)=0.23). **b-d:** Only pixels in air are shown (found by level-set segmentation). Arrows indicate artifacts.
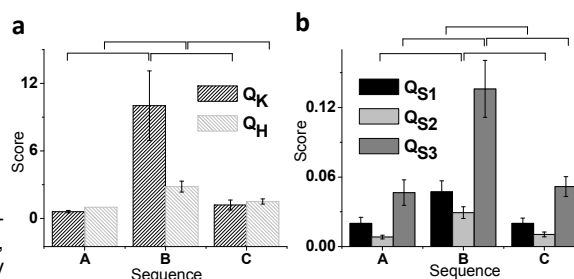
Fig. 2 Bar plots for Q_K and Q_H (**A**) and for the second method (**B**), grouped by sequence. Intervals on top indicate statistical significance of individual comparisons (P<0.05).

References: (1) Zhou et al., SCMR *2009* 3748; **(2)** Zhou et al., SCMR *2010*; **(3)** Mortamet et al., MRM 62:365-372 (2009); **(4)** Li et al., *IEEE CVPR 2005* (1)430-436.